

Enhancing Photocatalytic Activity of Dye Sensitized Solar Cell Counter Electrode Using Graphene Layers.

Kiplang'at M. Ng'eno¹, Mugo S. Waweru², Timonah N. Soita².

Abstract: Dye sensitized solar cells (DSSC's) were fabricated using graphene-based counter electrodes (CE's). The CE's were characterized using UV-Vis spectrophotometer and four point probe. From obtained transmittance spectra, single layer graphene, double layer graphene and platinum (Pt) on fluorine-doped tin oxide glass (FTO) exhibit high transmittance (above 70%) at visible wavelengths. Multi-layer graphene and Pt/multilayer graphene CE's showed a lower transmittance (below 70%). Transmittance reduces with increase in the number of graphene layers. Sheet resistance was found to reduce with increase in number of graphene layers: 1100, 520 and 180 Ω/sq for monolayer, bi-layer and MLG on FTO respectively. Photocurrent-voltage characteristics of the DSSC's were examined and the results showed incorporation of graphene (low R_s and high transmittance) could increase the short circuit current density and the photoelectric conversion efficiency (η). However incorporation of MLG (low R_s and high absorbance) led to reduction of η . Pt/single layer-Gr, pt/double layer-Gr, pt/multilayer graphene CE's had a conversion efficiency of 3.30, 3.41, and 2.16% respectively. Pt/double layer-Gr based CEs showed the highest conversion efficiency and improvement of 5.01% on η as compared to that of reference platinum based CEs

Key Word: Graphene layers, Platinum, counter electrode, dye sensitized solar cell.

Date of Submission: 02-03-2022

Date of acceptance: 17-03-2022

I. Introduction

Since the invention of DSSCs in 1991 by O'Regan and Gratzel, they have become so popular and promising new generation solar cells [1]. A lot of research has been done on DSSCs because of their low cost, light weight, moderate efficiency, flexibility and easy fabrication [2-4]. Typical DSSCs consist of a dye-sensitized semiconductor photoanode, an iodide/tri-iodide (I_3^-/I^-) redox electrolyte and a catalytic counter electrode. Counter electrode plays significant role of collecting electrons from external circuit and reducing I_3^- to I^- in the electrolyte. Fluorine doped tin oxide is usually loaded with platinum to facilitate electron transfer from the external circuit to the (I_3^-/I^-) redox electrolyte because of the high catalytic activity and conductivity of platinum [5]. However the combination between the limited resources of platinum and the large application of platinum based catalyst in the vehicle industry make the platinum extremely expensive and in diminishing supply. Therefore there is a need to explore pt-free materials to replace the pt counter electrode for DSSCs. Carbonaceous materials have been researched to be alternative candidates as CE because of their low cost, corrosion resistant and electrically conductive [6-8]. While graphite has poor catalytic activity towards the reduction of I_3^- , its high surface area analogs such as carbon black and carbon nanotubes, have been shown to be quite effective and in some cases even exceeded the performance of platinum. Graphene therefore has attracted a lot of attention because of its unique mechanical, thermal, electrical and optical properties [9-11]. As a 2D material graphene has a zero band gap material with a single molecular layered structure [11]. Each carbon atom of graphene uses 3 out its 4 outer orbital electrons to form 3 sigma bonds 120° a part with 3 adjacent carbon atoms in the same plane, leaving the forth electron to move. Electrons in graphene therefore behave as like massless relativistic particles without crystal lattices restrictions [12, 13]. Graphene possesses excellent electrical conductivities in two dimensions at room temperature [14].

This work present the effect of using pt on graphene layers as CE's on the conversion efficiency of DSSCs.

II. Material And Methods

In preparation of counter electrodes, CVD graphene layers (monolayer, bilayer and MLG, 1×1 cm, 95% coverage) on FTO, SnO₂: F, glass substrate (Graphene Supermarket Massachusetts, USA) were soaked in ethanol (99.5 % purity) for 5 minutes, rinsed with de-ionized water for 5 minutes and then dried with pressurized air. Cleaned Gr layers on FTO were used as CEs and some used in preparation of Pt/Gr CEs. In preparation of Pt/Gr based CEs, the adhesive tapes were placed on the edges of Gr on FTO to form guide in spreading the platinum precursor paste (platisol T/sp pore size, 15-20 nm, solaronix Switzerland) through the doctor blade procedure. The prepared samples were heated at temperature ramp of 5°/min up to 175°C, and then sintered at 450°C for 30 min to activate the platinum films. Samples were left to dry in the furnace. In preparation of Pt CEs, platinum was deposited on FTO (sheet resistance, 7 Ω /sq, Solaronix, Switzerland) using doctor blade procedure. Sheet resistance of graphene on FTO was evaluated using four point probe and transmittance spectra of prepared CEs obtained using UV-Vis spectrophotometer. For working electrode, TiO₂ thin films were prepared through sol-gel technique. FTO were cleaned using acetone (99.9 %), ethanol (99.5 %) and deionized water subsequently for 5 minutes in each step. FTO glass substrates were then dried using pressured air. The adhesive tapes were then placed on the edges of the FTO glass substrates to form guide for spreading the Titanium nanoxide T/sp (18% wt, 15-20 nm, solaronix Switzerland). The films were left at room temperature for 30 minutes. Prepared TiO₂ thin films then annealed at temperature ramp 1°/min from room temperature to 175°C, and then sintered at 450°C for 30 min in a furnace. Samples then left to cool in the furnace. Prepared samples then dye- sensitized through immersing them in 0.5 mM cis-diisothiocyanato-bis(2,2'-bipyridyl-4,4'-dicarboxylato)ruthenium (II) bis (tetrabutylammonium), the so called N719 dye for 24 hours to maximize dye loading. Dye-sensitized solar cells were assembled by sealing the dye-coated TiO₂ electrode with the prepared platinum-coated FTO, platinum on graphene and graphene on FTO counter electrodes using a dupont surlyln (meltonix 1170-25 solaronix) leaving a small space for the electrolyte introduction. The redox couple, iodine/triiodide, (Iodolyte HI-30, Solaronix, Switzerland) was then introduced into the space between the electrodes and later sealed. The fabricated solar cells were then characterized by analyzing the I-V characteristics obtained through applying an external bias on the cell in a dark room. A 450 W halogen lamp adjusted to an intensity of 100mW/cm² was used. The irradiance on the DSSCs was maintained at 1 sun, 100mW/cm² with the use of a solar power meter TM206 and single crystal Si photoanode. During characterization, the cells were covered with a black-printed paper with a hole measuring 1cm² for the active area. The photovoltaic (PV) parameters, open-circuit voltage (Voc) short-circuit current density, Jsc, and the fill factor (FF) were extracted from the I-V curve and used to calculate the DSSC's power conversion efficiency.

III. Result and Discussion

Optical properties of graphene based CEs.

The optical transmittance of monolayer, bi-layer and multi-layer graphene on FTO was measured at wavelength of 500-800nm, with offsetting to that of blank FTO. The transmittance is observed to increase with increase in the wavelength; however, with longer wavelengths of more than 700 nm, transmittance reduces. All samples show similar trend and optical transmittance is noted to reduce with increase in graphene layers on FTO as given in figure 1.

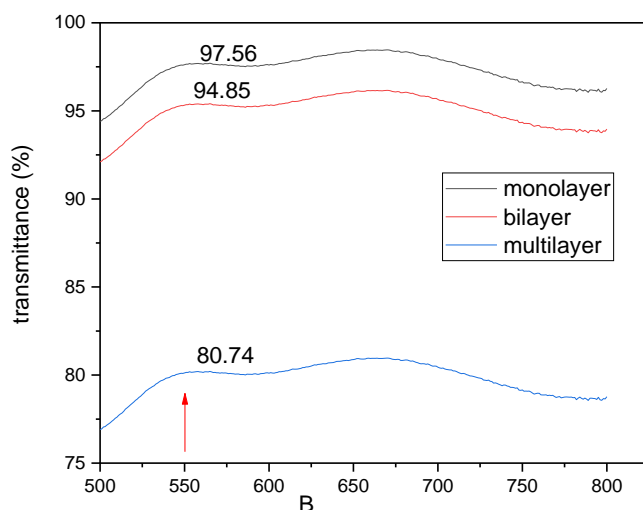


Fig. 1 transmittance of monolayer, bilayer and multi-layer Gr .

At normal incidence of 550 nm the transmittance of monolayer, double layer and multi-layer was found to be 97.56, 94.85 and 80.74 ± 0.005% respectively and these results agrees with numerical studies using equation 1 and reported work [15-17]. Monolayer graphene exhibit high transmittance with opacity of □ 2.4%, which is slightly higher than theoretical value of 2.3% (π α), which can be attributed to graphene’s unique electronic structure. Each layer increase in graphene layers corresponds to a decrease of 2.4% in the optical transmittance of these films. The number of graphene layers on MLG was determined using transmittance at 550 nm of 80.74% with the application of equation 1 to be 9.

$$T = [1 + 1.13\pi\alpha \frac{N}{2}]^{-2} \dots\dots\dots (1)$$

Where T is the transmittance, α is fine structure constant and N is the number of graphene layers. Transmittance spectra of bare FTO, single layer graphene, double layer graphene and multi-layer graphene layers on FTO CE’s was taken from 280 nm to 800 nm. Transmittance of all samples increases from wavelength of 300-800 nm. At shorter wavelengths, below 280 nm, the transmittance is observed to be low for all samples. Optical transmittance is noted to reduce with increase in graphene layers on FTO as shown in figure 2.

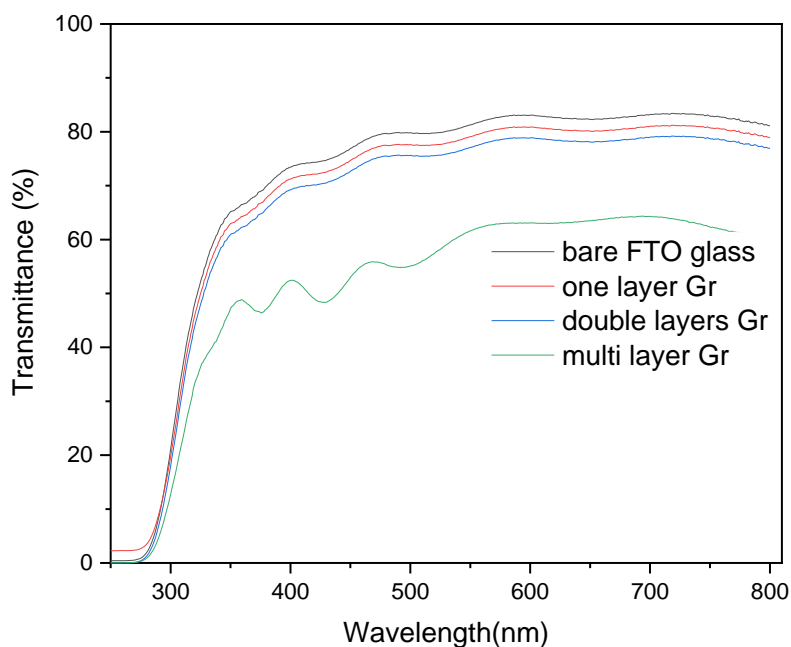


Fig. 2: Transmittance spectra of bare FTO glass, single, double and multi-layer graphene on FTO glass.

At wavelength □ 580nm all sample show maximum transmittance with bare FTO, monolayer, bi-layer and multi-layer on FTO having 83, 80, 78, and 60 % respectively. The transmittance of graphene was noted to drop with the increase in the number of layers, with multilayer graphene on FTO giving the lowest transmittance that is below 70 %. Single layer and bi-layer on FTO is highly transparent in the visible-UV range. High transmittance of few layers of graphene on FTO is significant for DSSC in allowing the movement of incident sunlight down to the active region of DSSC photoanode. Graphene can absorb light of wavelength range from 200 to 800nm and therefore the addition of graphene layers caused an increase of light absorbance thus reducing the transmittance as observed.

Platinum on graphene based CEs transmittance spectra was taken from 280-800nm and all samples exhibit similar trend. At shorter wavelength the transmittance is observed to be low. However with the change in wavelength 280-800 nm, the transmittance of all samples increases as shown in figure 3.

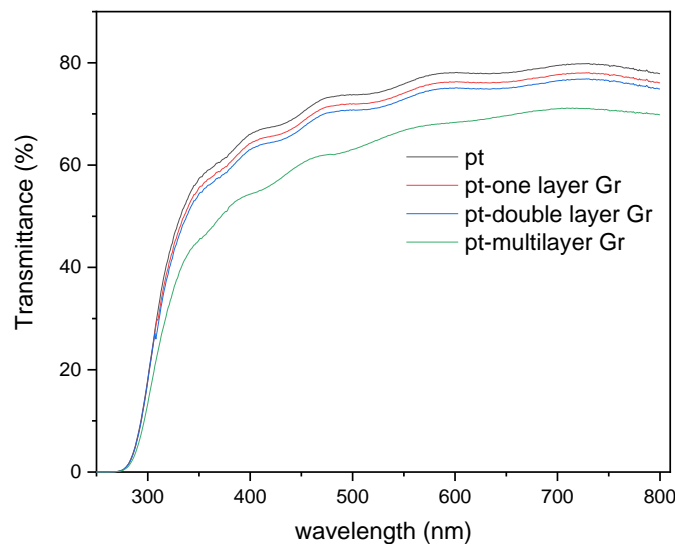


Fig.3: Transmittance spectra of bare FTO, platinum deposited on FTO, and on single, double and multilayer graphene using doctor blade method.

Platinum incorporated on graphene layers CE's showed a high transmittance more than 75 % at a visible range. Platinum on graphene layers does not also cause any optical interference as the transmission spectra exhibit a similar trend showing the slight reduction in transmission spectra. The high and constant transmittance of 70 % in the most of the visible range indicates that platinum on graphene layers CE's can be used for rear illumination and in window application.

Electrical properties

Sheet resistance of graphene on conductive substrate FTO was evaluated using four point probes by taking four equally spaced, co-linear probes (1 inch \times 1 inch) to make electrical contacts on graphene deposited on FTO. Direct current was applied between the outer two probes (1 and 4) and voltage drop is measured between the inner probes (2 and 3) then R_s calculated. Sheet resistance was observed to be high on single layer graphene on FTO and low on multi-layer graphene on FTO as given in figure 4.

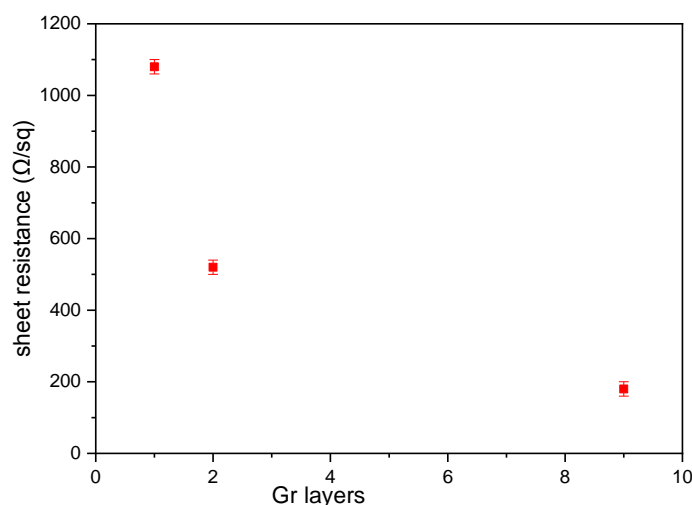


Fig.4: variation of R_s (Ω /sq) with graphene layers.

Sheet resistance of monolayer, bi-layer and multi-layer Gr on FTO is 1100, 520 and 180 Ω /sq respectively. From the results it can be noted that R_s reduces with increase in number of graphene layers. Reduction of R_s leads to increase in conductance of the films which is beneficial in photovoltaic application.

Photocurrent voltage curves for DSSCs fabricated from Pt, Pt/graphene layers based CE's are given in figure 5. The I-V curves obtained are noted to follow typical trend for DSSCs. Incorporating graphene on platinum based CE's is observed to affect J_{sc} , V_{oc} , FF and η of DSSCs.

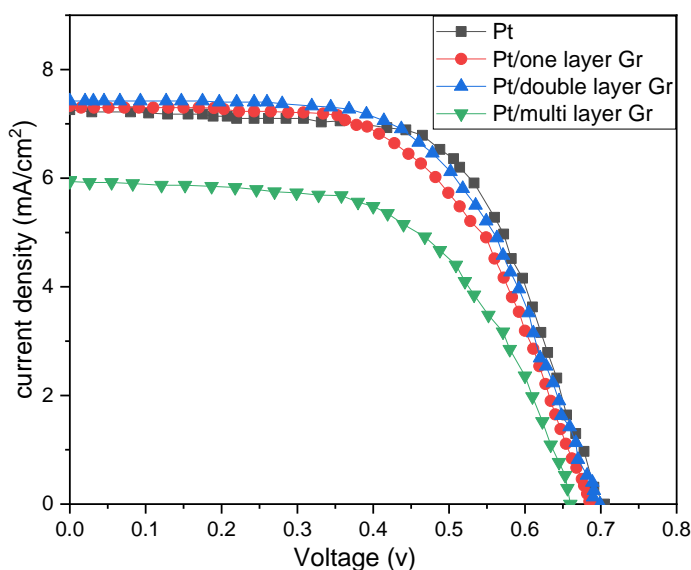


Fig 5: The photocurrent density-voltage curves of Pt/graphene layers CE's and reference Pt DSSCs.

All curves show similar trend with different photovoltaic parameters that are summarized in table 1. Few graphene layers on platinum based CE's is noted to improve on the FF, J_{sc} , V_{oc} , and η of DSSCs.

Table 1: Photovoltaic parameters Pt/graphene layers and Pt based CE's DSSCs.

Sample	V_{oc} (V)	J_{sc} (mA/cm ²)	F.F (%)	P_{max} (mW/cm ²)	η (%)
Pt	0.71	7.26	0.63	5.15	3.25
Pt/bilayer Gr	0.70	7.62	0.64	5.33	3.41
Pt/monolayer Gr	0.69	7.50	0.635	5.17	3.30
Pt/multi-layer Gr	0.66	5.96	0.55	3.93	2.16

The Pt based electrode, reference electrode, has open circuit voltage (V_{oc}), current density (J_{sc}), fill factor (FF), and efficiency of 0.71V, 7.26 mA/cm², 0.63 and 3.25% respectively. Pt on double layer Gr CE's was noted to improve J_{sc} , FF and η to 7.62 mA/cm², 0.64 and 3.41% respectively with slightly lower value of V_{oc} to that of Pt reference counter electrode. Comparing the maximum output power, Pt on bilayer Gr CE's gives the highest maximum power of 5.33 mW/cm². Pt on single layer Gr CE's improves J_{sc} from 7.26 to 7.50 mA/cm², FF slightly changing from 0.63 to 0.635 and also conversion efficiency improving from 3.25 to 3.30%. Incorporation of multi-layer Gr on Pt CE's, give relatively low values of V_{oc} , J_{sc} , FF and overall conversion efficiency. The observable difference in the DSSCs fabricated is on J_{sc} and PCE but there is no significant variation in both the V_{oc} and FF. Pt on few layer Gr, single and double layers, improve on the J_{sc} and hence on the overall conversion efficiency. This improvement can be attributed to high transmittance of both single layer and multi-layers of graphene films as observed. The conversion efficiency of DSSC is observed to increase with increase of graphene layers from monolayer to bi-layer then drop with MLG on Pt counter electrode. Incorporating single layer graphene on platinum improves η from 3.25 to 3.30% and double layer improve from 3.25 to 3.41%. Pt on double increases the conversion efficiency by \square 5%. Pt on multi layer graphene gives lower conversion efficiency as displayed in figure 6.

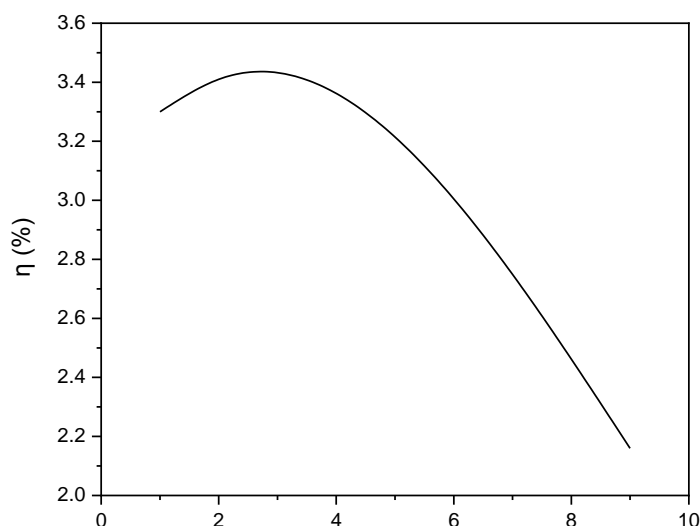


Fig.6: Variation of photo-current conversion efficiency with number of Gr layers loaded on Pt counter electrode.

Surface resistance of the graphene sheets is very important in an electrochemical cell, as sheet resistance determine the resistance of the electrons in the cell, influencing directly on the efficiency of the DSSC. As noted from the results above, with the reduction of sheet resistance, from 1100 to 520 Ω /sq, the conversion efficiency of solar cells of graphene on platinum based CEs, improves from 3.30 to 3.41%. MLG on FTO was noted to have improved Rs of 180 Ω /sq but conversion efficiency was found to be low, 2.16%, which can be attributed to low transmittance (insolation) as compared to single and double layers Gr. The low PCE could also be due to the establishment of graphene agglomerates in MLG in the CEs and these agglomerates act as trapping sites and provide the resistance to electrons, thus reducing current-density and overall efficiency [18].

From theory, the addition of graphene sheets increases the contact surface area of Pt particles on the cathode enhancing the efficiency of DSSCs [19, 20]. Additionally graphene is conductive as Pt; the addition of graphene layers improved the conductivity of the cathode, leading to the fast reaction kinematics in the reduction of I_3^- and the decrease of charge recombination [19, 21]. Higher efficiency of Gr/Pt based CEs demonstrates high electro-catalytic activity for I_3^- reduction. Incorporation of graphene to platinum increases availability of the metal particles for electron transfer. Furthermore, graphene could also provide a fast diffusion pathway for the electrolyte and ensure excellent electrode–electrolyte contact, which improves the electron transfer rate at the interface [22].

Gr CEs have been reported to have low FF which is a result of poor catalytic activity in the junction of graphene CE and the electrolyte arising from large charge transfer resistance (R_{CT}) [23-25]. High R_{CT} in the graphene - electrolyte interface is attributed to Poor diffusion of the I^-/I_3^- redox species in the pores of graphene hence the low FF [25]. The large R_{CT} leads to longer redox reaction times in the graphene CE hence amplification of charge recombination between electrons excited from the dye to the conduction band of TiO_2 and the I_3^- ions [23]. The low FF causes a potential drop across the graphene/FTO interface due to sluggish electron transfer leading to a low PCE [25].

IV. CONCLUSION

Sheet resistance of graphene films improves with increase in graphene layers; 1100, 520 and 180 Ω /sq for monolayer, bi-layer and MLG Gr on FTO respectively. Transmittance of Gr films reduces with increase in Gr layers. Pt does not cause any optical interference on the transmittance of Gr layers on FTO. Improved sheet resistance and high transmittance of graphene on FTO films was found to improve short circuit current density, fill factor and overall photocurrent conversion efficiency of DSSCs. Pt on double layer-Gr based CEs showed the highest conversion efficiency and improvement of 5.01% on η as compared to that of reference platinum based CEs. Higher efficiency of Gr/Pt based CEs demonstrates high electro-catalytic activity for I_3^- reduction. Incorporation of graphene to platinum increases availability of the metal particles for electron transfer.

However an incorporation of MLG graphene (low Rs and transmittance) reduces Jsc, FF and the overall performance of the solar cell.

REFERENCES

- [1]. B. O'Regan, M. Graetzel. A low-cost, high-efficiency solar cell based on dye-sensitized colloidal TiO₂ films. 353 (1991) 737-740.
- [2]. Z. Han, Z. Zhao, Z. Du, L. Zhao, X. A novel anode material of TiCl₄ treatment Ag/TiO₂ in Dye Sensitized Solar Cell. 136 (2014) 424-426.
- [3]. Y. Yang, X. Peng, S. Chen, L. Lin, B. Zhang, Y. Feng. Performance improvement of dye-sensitized solar cells by introducing a hierarchical compact layer involving ZnO and TiO₂ blocking films. 40 (2014) 15199-15206.
- [4]. D.D. Babu, S.R. Gachumale, S. Anandan, A.V. Adhikari. New D-π-A type indole based chromogens for dye sensitized solar cell. 112 (2015) 183-191.
- [5]. W. Sun, X. Sun, T. Peng, Y. Liu, H. Zhu, S. Guo, X.-z. Zhao. A low cost mesoporous carbon/SnO₂/TiO₂ nanocomposite counter electrode for dye-sensitized solar cells. 201 (2012) 402-407
- [6]. Kay A, Graetzel M. Low cost photovoltaic modules based on dye sensitized nanocrystalline titanium dioxide and carbon powder. 1996; 44:99-117
- [7]. Wroblowa HS, Saunders A. Flow-through electrodes: II. The I_3^-/I^- redox couple. *Electroanal Chem Int Electrochem* 1973; 42:329-46.
- [8]. Tarasevich MR, Khrushcheva EI. *Modern aspects of electrochemistry*. 2nd ed. New York: Plenum; 1989. 19
- [9]. C. H. Ng, H. N. Lim, S. Hayase, I. Harrison, A. Pandikumar, and N. M. Huang. Potential active materials for photo-supercapacitor. 296, 169 (2015).
- [10]. Y. H. Ng, I. V. Lightcap, K. Goodwin, M. Matsumura, and P. V. Kamat. To What Extent Do Graphene Scaffolds Improve the Photovoltaic and Photocatalytic Response of TiO₂ Nanostructured Films? 1, 2222 (2010).
- [11]. R. Nair, P. Blake, A. Grigorenko, K. Novoselov, T. Booth, T. Stauber, N. Peres, and A. Gein. Fine structure constant defines visual transparency of graphene. 320, 1308 (2008).
- [12]. S. Stankovich, D. A. Dikin, G. H. Dommett, K. M. Kohlhaas, E. J. Zimney, E. A. Stach, R. D. Piner, S. T. Nguyen, and R. S. Ruoff. Graphene-based composite materials. 442, 282-286 (2006).
- [13]. D. Li and R. B. Kaner. Graphene-based materials. 320, 1170 (2008).
- [14]. Y. Si and E. T. Samulski. Synthesis of water soluble graphene. 8, 1679 (2008).
- [15]. Sheehy DE, Schmalian J. Optical transparency of graphene as determined by the fine-structure constant. *Phys Rev B* 2009;80:193411-4.
- [16]. Zhu SE, Yuan SJ, Janssen GCAM. Optical transmittance of multilayer graphene. *EPL (Europhys Lett)* 2014;108 (1):17007.
- [17]. Bruna M, Borini S. Optical constants of graphene layers in the visible range. *Appl Phys Lett* 2009;94:031901-3
- [18]. Umer M., Hafza A., Falak B., Muhammad Y. Effect of graphene contents in polyaniline/graphene composites counter electrode material on the photovoltaic performance of dye-sensitized solar cells., 2019, 196, 132-136.
- [19]. N. T. Khoa, D. V. Thuan, S. W. Kim, S. Park, T. V. Tam, W. M. Choi, S. Cho, E. J. Kim, S. H. Hahn. Facile fabrication of thermally reduced graphene oxide-platinum nanohybrids and their application in catalytic reduction and dye-sensitized solar cells, *RSC Adv.*, 2016, 6(2), 1535-1541.
- [20]. A. B. Suriani, Fatiatun, A. Mohamed, Muqoyyanhah, N. Hashim, M. S. Rosmi, M. H. Mamat, M. F. Malek, M. J. Salifairus, H. A. Khalil. Reduced graphene oxide/platinum hybrid counter electrode assisted by custom-made triple-tail surfactant and zinc oxide/titanium dioxide bilayer nanocomposite photoanode for enhancement of DSSCS photovoltaic performance, *Optik*, 2018, 161, 70-83.
- [21]. D. Tasis. Recent progress on the synthesis of graphene-based nanostructures as counter electrodes in DSSCs based on iodine/iodide electrolytes, *Catalysts*, 2017, 7(8), 234.
- [22]. Cheng C., Lin C., Shan C., Tsai S., Lin K., Chang C. and Chien S. Platinum-graphene counter electrodes for dye sensitized solar cells", *Journal of Applied Physics*, Vol. 114, pp. 014503, 2013.
- [23]. Y. Y. Dou, G. R. Li, J. Song and X. P. Gao. Nickel phosphide-embedded graphene as counter electrode for dye-sensitized solar cells. 2012, 14, 1339-1342.
- [24]. Jeng M., Wung Y., Chang L. and Chow L. Particle size effects of Tio2 layers on the solar efficiency of dye-sensitized solar cells", *International Journal of Photoenergy*, Vol. 2013, pp. 563897, 2013.
- [25]. Yang W., Xu X., Tu Z., Li Z., You B., Li Y. Raj S.I., Ynag F., Zhang L., Chen S., Wang A., Nitrogen plasma modified CVD grown graphene as a counter electrodes for bifacial dye-sensitized solar cells, *Electrochimica Acta*, Vol. 173, pp. 715-720, 2015.

Kiplang'at M. Ng'eno, et. al. "Enhancing Photocatalytic Activity of Dye Sensitized Solar Cell Counter Electrode Using Graphene Layers." *American Journal of Engineering Research (AJER)*, vol. 11(03), 2022, pp. 01-07.